Available online at www.CivileJournal.org

Civil Engineering Journal

Vol. 5, No. 1, January, 2019

Simple Equations for Considering Spatial Variability on the Bearing Capacity of Clay

Davood Azan [a*], Abdolhosein Haddad [b]

[a] PhD Candidate, Faculty of Civil Engineering, Semnan University, Semnan, 35131-19111, I.R. Iran.

[b] Associate Professor, Faculty of Civil Engineering, Semnan University, Semnan, 35131-19111 I.R. Iran.

Received 26 September 2018; Accepted 13 December 2018

Abstract

In the present paper, the effect of spatial variability of undrained shear strength on the bearing capacity of shallow strip footing on clay was investigated and two new and simple equations were introduced for incorporating the effect of soil variability parameters on the undrained bearing capacity of strip footing on clay. For investigating the spatial variability of clay, undrained shear strength was assumed as a spatial variable parameter with the use of random field theory. The Monte Carlo simulation technique was used to obtain the probability distribution of the bearing capacity of footing on nonhomogeneous clay. The spatial variability of the undrained shear strength was investigated using three controlling parameters: coefficient of variation (COV) of the undrained shear strength as well as the scales of fluctuation of the shear strength in horizontal and vertical directions. The Mohr-Coulomb failure criterion and finite difference method were used to model the plastic behaviour of soil and calculate the bearing capacity of the footing. The results show that by increasing the COV of the undrained shear strength, the average bearing capacity decreases while the COV of the bearing capacity increases. Moreover, the average bearing capacity of footing has an approximate increasing trend with increasing the scales of fluctuation.

Keywords: Bearing Capacity; Spatial Variability; Monte Carlo simulation; Finite Difference Method; Multiple Regression Analysis.

1. Introduction

The existing uncertainty in the mechanical response of soil to the applied loading originates from the spatial variation of soil properties. This uncertainty is a well-known problematic issue for the accurate design of soil-related structures. The random field theory (RFT) is an ordinary tool for applying the spatial variation of soils [1-5]. This theory has been utilized for formulating spatial variability of soil in geotechnical engineering problems. Estimating the bearing capacity of footings on heterogeneous clay soil is a geotechnical problem in which consideration of spatial variability of underlying clay layers has an important effect on the results. Although the effect of spatial variability has been investigated on the bearing capacity of clay layers in some previous studies [6-20], there has been no study that comprehensively considered the effect of spatial variability parameters on the bearing capacity of footings on clay.

Griffiths and Fenton (2001) investigated the bearing capacity of smooth footings on clay by considering the spatial variability of undrained shear strength. They implemented the finite element method with Tresca yield criteria to calculate the bearing capacity of smooth footings. In their study, the logarithmic normal distribution was used for shear strength distribution in the random field. They used the coefficient of variation (COV) of undrained shear strength (COV(c_u)) and the ratio of the scale of fluctuation to the width of footing (θ_{lncu} /B) to study the effect of spatial variability

* Corresponding author: azan_davood@semnan.ac.ir

http://dx.doi.org/10.28991/cej-2019-03091228

of clay on the bearing capacity of footings. They implemented the Monte Carlo simulation (MCS) to obtain a probabilistic distribution. In their study, scales of fluctuation (θ_{lncu}) were assumed to be equal in horizontal and vertical directions. However, in their study, the scales of fluctuation in horizontal and vertical directions were not investigated as two distinct and independent parameters. They concluded that the average bearing capacity from the MCS constantly decreased with the increase of COV(c_u); moreover, by growing of the (θ_{lncu}/B) ratio, the bearing capacity of footing decreased when this ratio was lower than unity but increased when the ratio exceeded unity [10]. Griffiths et al. (2002) investigated the effect of spatial variability of soil undrained shear strength on the bearing capacity of rough footings. They used the same parameters as Griffiths and Fenton (2001) to investigate the effect of spatial variation of soil on the bearing capacity of clay. They concluded that the effect of spatial variability of soil on the bearing capacity of rough footings was the same as that on smooth footings [11]. Jamshidi Chenari and Mahigir (2014) investigated the effect of spatial variability and anisotropy of soil on the bearing capacity of shallow strip footings. In their study, the finite difference method (FDM) was implemented for calculating the bearing capacity, and Mohr-Coulomb failure criteria were utilized to consider the mechanical response of soil to loadings. Similar to Griffiths and Fenton (2001), they used log-normal distribution to consider the spatial variability of soil undrained shear strength. They also did not investigate the effect of scales of fluctuation on the bearing capacity of footings in horizontal and vertical directions separately. They used two parameters (i.e., Cov(c_u) and the ratio of scale of fluctuation in x and y directions (θ_x/θ_y) to study the effect of spatial variability of the shear strength parameter on the bearing capacity. Like previous studies, the reduction in the average bearing capacity with the increase in Cov(c_u) was concluded. In addition, the average bearing capacity was observed to increase by the growth of the (θ_x/θ_y) ratio [17]. As indicated, there has been no study to examine comprehensively the effect of spatial variability parameters especially the scales of fluctuation θ_x and θ_y on the bearing capacity of footings on heterogeneous clay soils. Therefore, in this research, a parametric study is carried out to assess the effect of changing θ_x and θ_y values on the bearing capacity of strip footings located on purely cohesive clay. For calculating the bearing capacity, the FDM with the Mohr-Coulomb failure criteria is implemented using FLAC 7.0 [21]. Three parameters of Cov(c_u) θ_x/B,θ_y/B (in which B is the footing width) with proper ranges are investigated in a parametric study and subsequently, the effect of changes in these parameters is assessed on the bearing capacity. Ultimately, two new and simple equations are proposed to estimate the average bearing capacity and scattering of the results from average by using multiple regression analysis (MRA)[22]. These equations can be used easily to consider soil spatial variability in the design of strip footings on nonhomogeneous clay.

2. Spatial Variation of Soil

One of the major characteristics of geological conditions of a site is depicted in soil deposits available in the site. Soil layers are largely formed due to gradual weathering as well as due to the erosion of rocks and sedimentation of solid earth materials. Soil deposits except residual soils are transported from the origin to the current position and are subjected to pore pressure variations, physical changes and/or chemical reactions; hence, variation in soil properties from one location to another is natural in the field. Variation of soil properties in the field is called spatial variation of soil properties and it is an important issue in the analysis and design of soil-related structures [8].

In engineering problems, modelling of spatial variations of geotechnical properties has commonly been performed using the RFT. In the RFT, soil properties are assumed as correlated random numbers and subsequently, the distribution of soil properties in the field is modelled. Figure 1 schematically depicts spatial variation of soil properties using the RFT. In this figure, soil variations are assumed to occur in two perpendicular directions (i.e., x and y directions), and the values of soil properties fluctuate from the average regarding the characteristics of the assumed distribution and autocorrelation function.

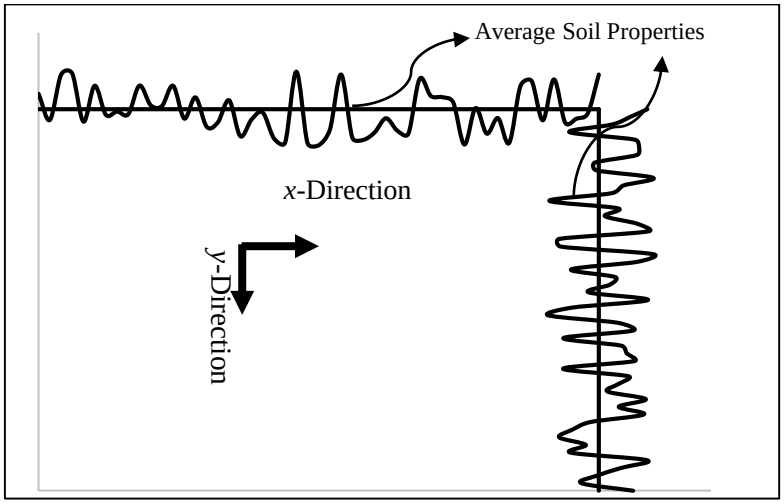

Figure 1. The schematic view of distribution of soil parameters by applying the random field theory

In this research, it is assumed that the soil undrained shear strength is distributed in the field using the RFT. Since the variations related to the bearing capacity of the undrained shear strength is investigated, to present the results of the current study, the undrained shear strength coefficient (N_C) in classical bearing capacity equations is chosen [22]. N_C can be calculated using:

$$N_c = \frac{q_u}{c_u} \quad (1)$$

Where q_u is the ultimate bearing capacity of the shallow strip footing and c_u is the undrained shear strength of clay.

Since the average shear strength of clay is assumed as a constant value, there is a linear relationship between N_C and the bearing capacity of clay. Thus in this study, two terms of "bearing capacity" and "shear strength coefficient in classical bearing capacity equation (N_C)" are assumed equivalent and used interchangeably. As the shear strength of clay is always a positive value, in this research, lognormal distribution is assumed to generate a random field. Moreover, as noted, since N_C is used to present the results of the current study, the values of c_u do not affect the results; thus, for log-normal distribution, the average undrained shear strength is assumed to be a constant value. Subsequently, to consider the scatter in the parameters, the COV, which is a non-dimensional ratio, is chosen instead of the standard deviation (σ). This ratio is:

$$COV = \frac{\sigma}{\mu} \quad (2)$$

Where μ and σ are the average and standard deviation of the distribution.

Spatial autocorrelation between the shear strength values in the field is another characteristic of spatial variability that must be regarded in order to generate a random field. As is obvious in realistic field problems, two locations that are near each other are more probable to have closer shear strength values. In other words, shear strength values have greater correlation in two locations that are close to each other. The correlation between shear strength values for two points in the field is assumed to be just within autocorrelation length (or scale of fluctuation). Scale of fluctuation or autocorrelation length is a distance within which shear strength values correlate with each other; when the distance of two points in the space exceeds autocorrelation length, the correlation diminishes between shear strength values of the two points.

In the present study, the correlation for the shear strength values is assumed in both *x* and *y* directions; thus, for this purpose, the Markovian spatial correlation function which is presented in Equation 3 is implemented. This correlation function has been commonly used in geotechnical engineering problems [12].

$$\rho = \exp(-2\sqrt{\left(\frac{\tau_x}{\theta_x}\right)^2 + \left(\frac{\tau_y}{\theta_y}\right)^2}) \quad (3)$$

In this equation, θ_x and θ_y are scales of fluctuation in horizontal and vertical directions; moreover, τ_x and τ_y are matrices for lag distances in *x* and *y* directions. As the shear strength has log-normal distribution, $\ln(c_u)$ can be calculated using the following equation:

$$\ln(c_u) = L.\varepsilon + \mu_{\ln c_u} \quad (4)$$

Where $\mu_{\boldsymbol{ln\,cu}}$ is the average of $\ln(c_u)$, $\boldsymbol{\varepsilon}$ is a Gaussian vector (with zero mean and unit variance), and **L** is a lower triangular matrix, which can be computed using the following equation:

$$T = L.L^T \quad (5)$$

where T is covariance matrix; this matrix can be calculated using a given covariance function. In this study, the isotropic covariance function of Equation 6 is implemented.

$$T = \sigma^2_{\ln c_u} \exp(-2\sqrt{\left(\frac{\tau_x}{\theta_x}\right)^2 + \left(\frac{\tau_y}{\theta_y}\right)^2}) \quad (6)$$

In this equation, $\sigma_{\ln c_u}$ is the standard deviation of $\ln(c_u)$; other parameters of this equation are introduced in Equation 3.

3. Numerical Modelling

3.1. Modelling Configurations and Solution Algorithm

As noted, for computation of the bearing capacity, the FDM is implemented using FLAC7.0. Geometry, boundary conditions of the modelling, as well as the finite difference grid, which is used for computation of the bearing capacity, are illustrated in Figure 2. As shown in this figure, the distances of the vertical boundaries from the footing edges are $4.5B$ and the vertical distance between the bottom boundary and footing is $10B$. These distances are chosen so that the boundary conditions do not affect the obtained numerical results. For consideration of geostatic stress conditions in

practical field problems, the displacements of the vertical boundaries are fixed in the horizontal direction, while displacements of the bottom boundary are fixed in both the horizontal and vertical directions. The footing is considered rigid and perfectly rough. This is done by restraining vertical and lateral movements of nodes beneath the footing and applying step-by-step vertical displacements to the nodes under the footing. As is shown in Figure 2 the finite difference grid is divided into 50 elements in both horizontal and vertical directions thus the grid consists of 2500 square elements and 2601 grid points.

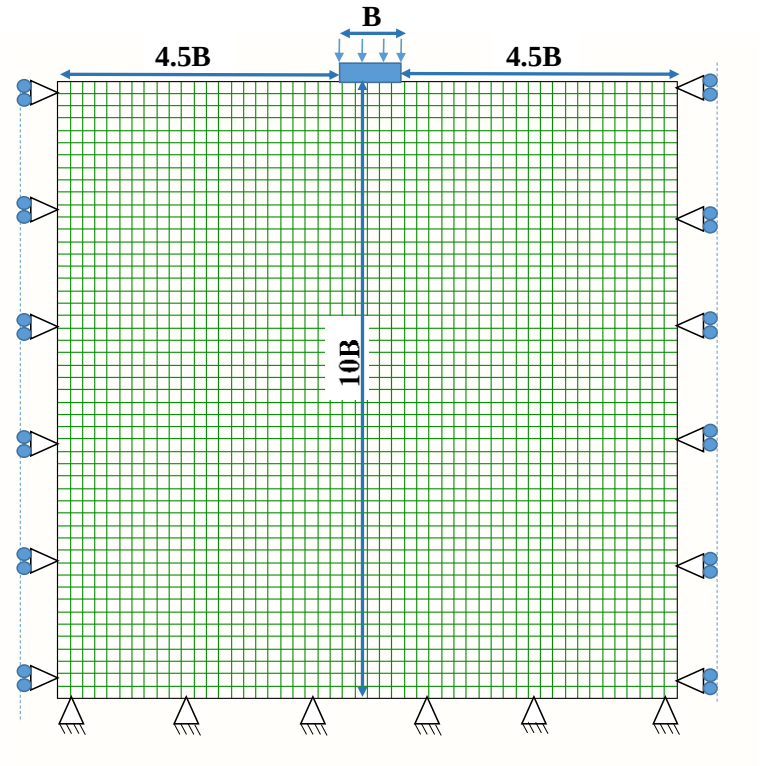

Figure 2. The geometry and boundary conditions and grid for the numerical model

Figure 3 shows the flowchart of the steps used for the numerical modelling in this study. For consideration of spatial variation of the undrained shear strength, initial values used for the studied parameters must be inserted into the modelling code. Afterwards, by considering the lognormal distribution, correlation function and values for the COV of the shear strength, the matrix is calculated for the shear strength values of the grid. Finally, by applying step-by-step vertical displacements to the nodes under the footing as well as by monitoring vertical nodal forces and plotting a stress-displacement graph, failure load, which is the ultimate bearing capacity of the footing, will be determined.

A schematic graph for average vertical stress versus vertical displacement of the nodes under the footing is illustrated in Figure 4. Since the constitutive model that is used to study the mechanical behavior of soil to the loading is elastic perfectly plastic Mohr-Coulomb, the plot comprised of two distinct parts (i.e. elastic and plastic). When the shape of the load-displacement curve switches from a declined curve to a horizontal line, the relevant vertical load in this step will be recorded as the ultimate bearing capacity (q_u). In this stage, a failure zone forms under the footing. In the failure zone, the points are in the plastic state. Figure 3 represents a typical example of failure zone under the footing from the analyses of the current study. In this figure, the red stars and green crosses show the grid elements where are in elastic and plastic states respectively.

The steps from the generation of shear strength matrix to calculation of bearing capacity should be repeated until a proper statistical population is obtained. This statistical population is employed to establish a probabilistic distribution. Subsequently, the average and COV of the distribution will be calculated.

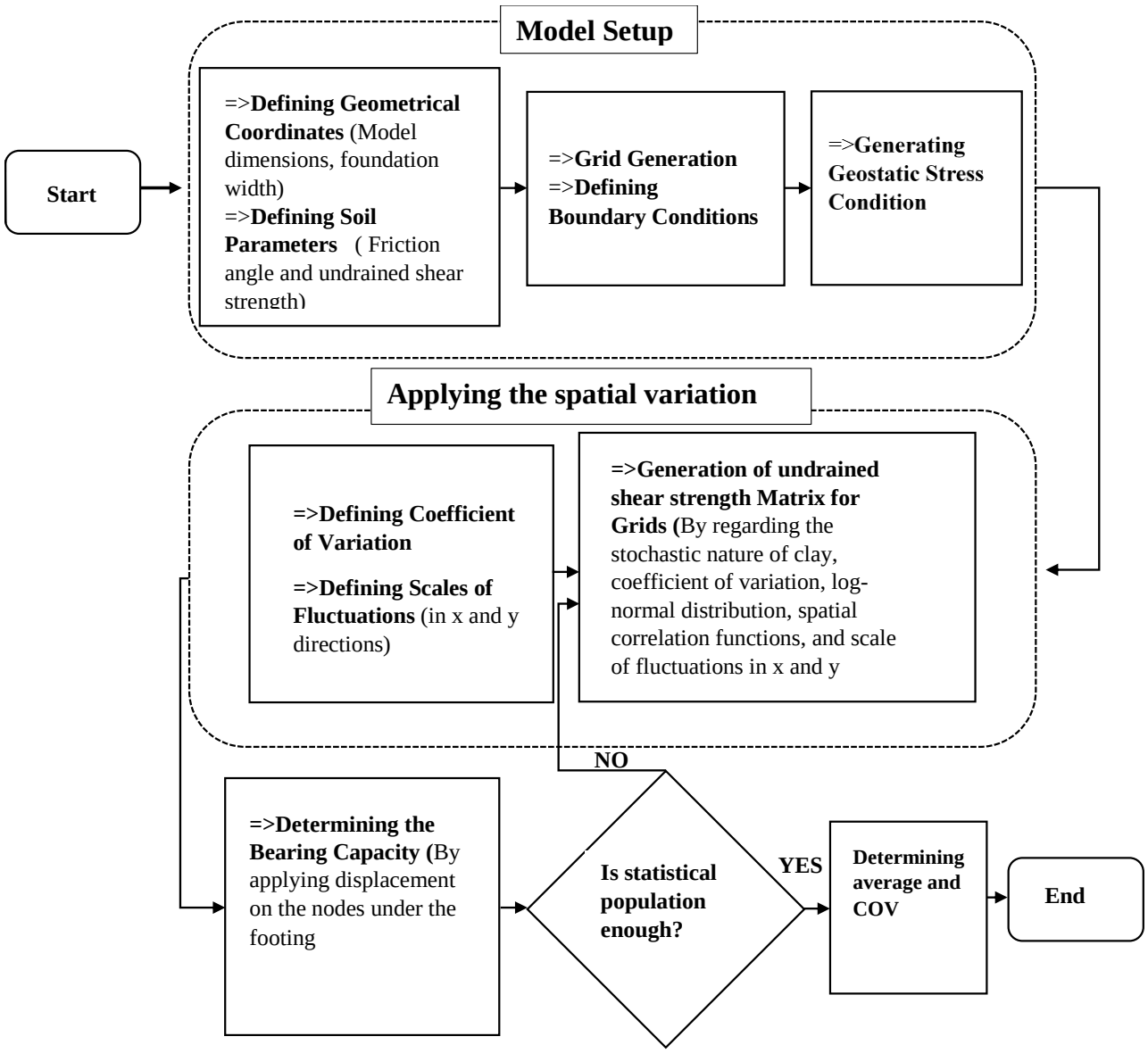

Figure 3. The flowchart of determination of the bearing capacity of foundation on clay by consideration of spatial variability of the shear strength

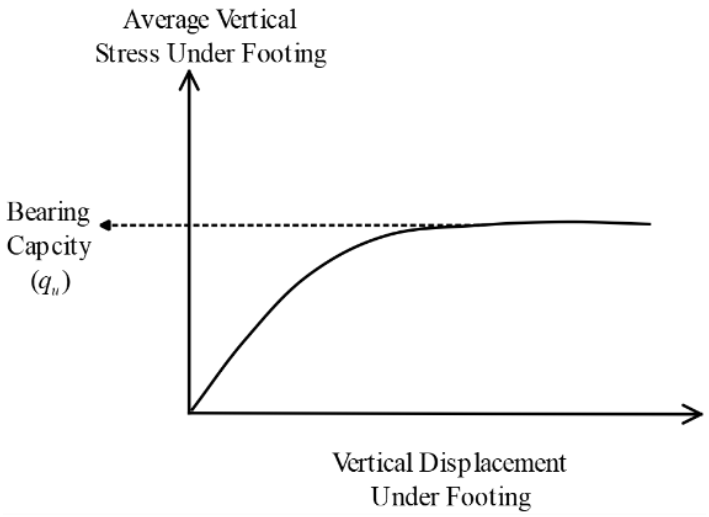

Figure 4. Average stress vs. vertical displacement under the footing curve

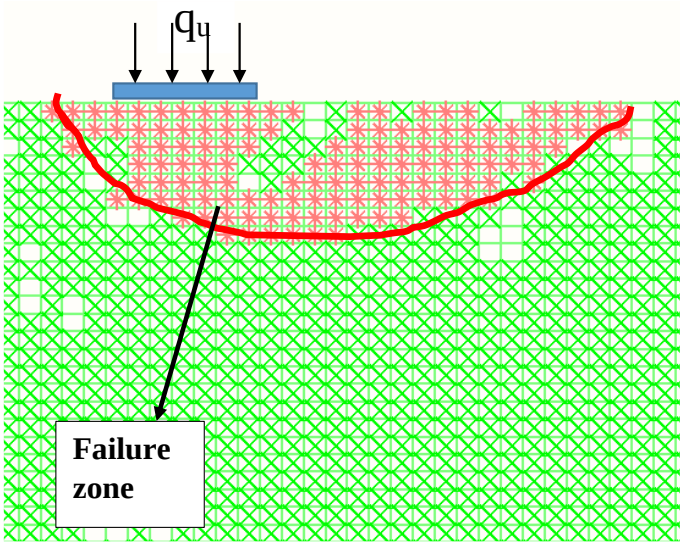

Figure 5. Failure zone formed under footing at the bearing capacity of soil

4. Verification of the Results

For primary verification of the results of the current study, one model is located on homogeneous clay soil to calculate the bearing capacity of the shallow strip footing and the result of this analysis is compared with the results of classical bearing capacity formulations (i.e., Terzaghi, Hansen and Meyerhof equations) [23]. As is known, the effect of parameters such as elastic modulus, Poisson ratio, soil unit weight and footing width (B) are negligible in determining the undrained bearing capacity of the shallow strip footing resting on cohesive clay. For cohesive clay in undrained state, the friction angle is zero; however, for convergence requirements of numerical analysis, the friction angle is given a small value close to zero. The constant parameters used in the analyses are listed in Table 1[24].

Table 1. The constant parameters used in this research

Parameter	Numerical Value
Average Undrained Shear Strength(KN/m^2)	10
Foundation Width(m)	2
Unit Weight(KN/m^3)	17
Elasticity Modulus	300.c_u
Poisson Ratio	0.49
Friction Angle(^{o})	Close to zero

In Table 2, the results obtained from the current study are compared with the results of common classical bearing capacity formulations. It is observed that the numerical results of the current study are equal to classical equations.

Table 2. Verification of N_C values of the current study for footing on homogeneous clay

Bearing Capacity Equation	N_C
Terzaghi	5.7
Hansen	5.1
Meyerhof	5.1
Current Study	5.1

3.2. The Parametric Study

As indicated earlier in this study, the COV of the undrained shear strength $COV(c_u) = \sigma_{cu}/\mu_{cu}$ is used to represent the level of scatter in the undrained shear strength. The inspected parameters in the current parametric study are COV(c_u), θ_x and θ_y. Reasonable ranges are selected for these three parameters so that the results obtained from the current study can be generalized to any empirical field conditions and can be used in the design of strip footings located on the clay layers with the specified degree of variability. Since the scales of fluctuation of soil act with respect to the footing width, the non-dimensional ratios of θ_x/B and θ_y/B are used in the parametric study.

The studied parameters and their numerical values are presented in Table 3.

Table 3. The parameters under investigation and their numerical values

Parameters	Numerical Values
COV_{c_u}	0, 0.2, .., 1
θ_x/B	0.5, 1, 2, 3
θ_y/B	0.5, 1, 2, 3

For illustrating the effect of the scales of fluctuation on the shear strength contours of the model, two cases are shown for the shear strength contours with different θ_x/B and θ_y/B ratios (Figure 6). In these figures, ratios of θ_x/B and θ_y/B are chosen to be equal and the COV(c_u) is constant (COV(c_u)=0.8). It should be noted that the parameters are assumed in order to show the spatial variability of shear strength in a better way.

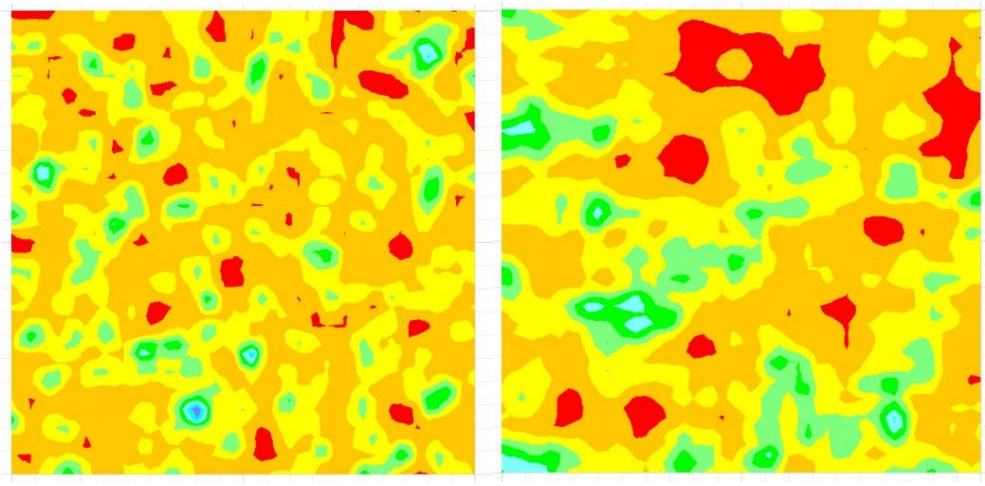

(a) **(b)**

Figure 6. The shear strength contours for the model for Cov(c_u)=0.8 and equal scale of fluctuation in x and y directions a) 0.2, b) 0.8

For choosing the optimum number of analyses so that the average of the results approximately converges to a constant value, a specified case of the bearing capacity problem is investigated. The properties for the spatial variation parameters of the shear strength in this problem are listed in Table 4. In this model, the MCS is performed with 1000 analyses; after each analysis, the average of statistical population and its COV are calculated. Then, these values are plotted against the number of analyses. Figures 7 and 8 indicate the variations of the average N_C and its COV with increasing the number of analyses in the MCS.

Table 4. The parameters and their numerical values in the analysis

Parameters	Numerical Value
μ_{c_u}(Kpa)	10
Cov(c_u)	0.6
θ_x/B	1
θ_y/B	1

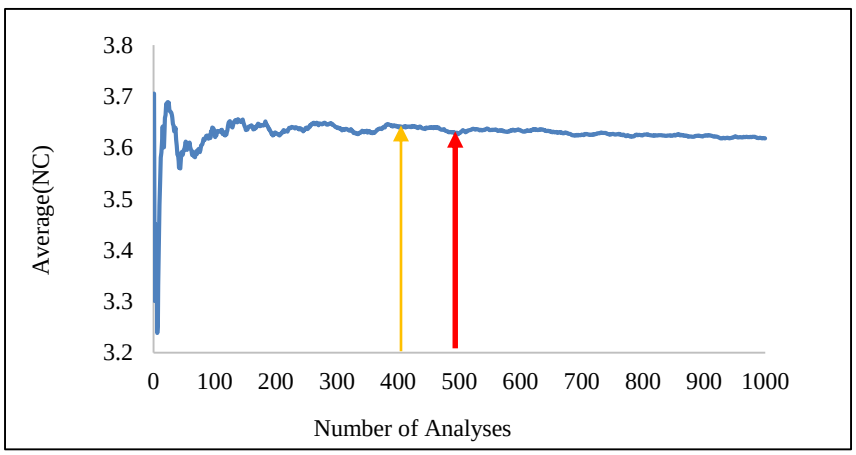

Figure 7. Variation of the average N_C with increasing the number of analyses in the MCS

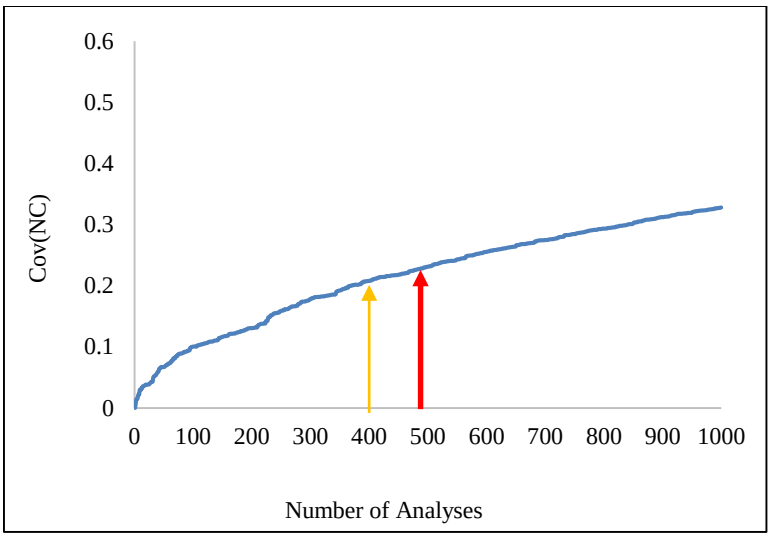

Figure 8. Variation of the COV of N_C with increasing the number of analyses in the MCS

It can be interpreted from Figures 7 and 8 that after 400 analyses in the MCS, the average statistical population and its COV approximately converges to a constant value. This number of analyses can be considered as the adequate number of analyses in the MCS for the current study. However, to achieve the results with higher degree of confidence, in the current study, the standard number of analyses in the MCS is set to be 500.

5. Results

By performing the MCS with 500 analyses for each group of parameters, the probability density functions (PDFs) are plotted. Figure 9 shows the PDFs for COV(c_u)=0, 0.2, …, 1. In this figure, the values of θ_x/B and θ_y/B are assumed to be constant ($\theta/B = \theta_y/B = \theta_x/B$=1.0). It is observed that with the increase in COV(c_u), the bell-shaped PDFs become wider and also the peak values of the PDFs tend to smaller quantities. From this observation, it can be interpreted that by growing the COV(c_u), the average values of N_C (Average(N_C)) reduce while the variance or scatter in N_C values grow larger; therefore, by increasing the COV(c_u), the degree of confidence in the Average(N_C) decreases.

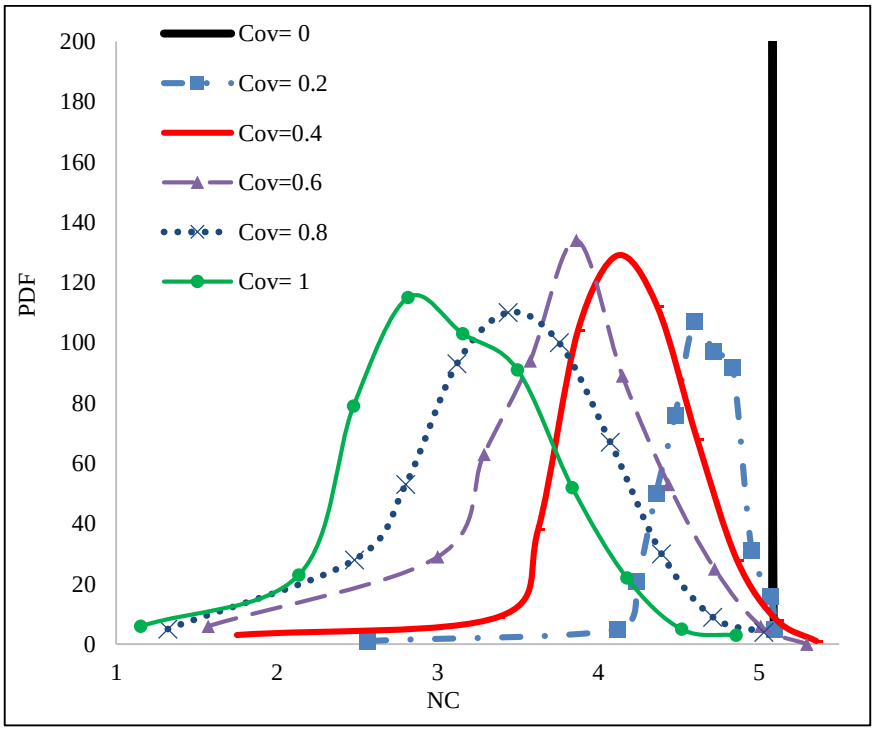

Figure 9. Probability density functions of N_C for different COV values

5.1. Effect of Scales of Fluctuation

In Figures 10 and 11, the variations of Average (N_C) are drawn vs. Cov(c_u) for different ratios of θ_x/B and θ_y/B respectively. As expected in all of the curves, Average (N_C) decrease with the increase in Cov(c_u). In Figure 10, it is observed that when θ_x/B is constant, the rate of reduction of Average (N_C) with the increase in Cov(c_u) is higher when

θ_y/B ratios are lower. This trend is seen in all of the curves of Figure 10. However, the Average (N_C) values are approximately the same in $\theta_y/B = 2$ and $\theta_y/B = 3$. In Figure 11, in spite of some exceptions, the Average (N_C) decreases at a higher rate when θ_y/B ratios are higher; this is the same trend as in Figure 10. By observing the Figures 10 and 11, it can also be interpreted that by the increase in θ_x/B and θ_y/B , the maximum reduction in the Average(N_C) values increases. Therefore the lowest value of Average (N_C) is 3.4 that occurs when θ_y/B and θ_x/B are 3. Thus, the maximum reduction in undrained bearing capacity due to spatial variation of shear strength is expected to be 33.3 percent. Considering this amount of reduction in the bearing capacity studies can be very effective in the safe design of strip footings resting on heterogeneous clay layers.

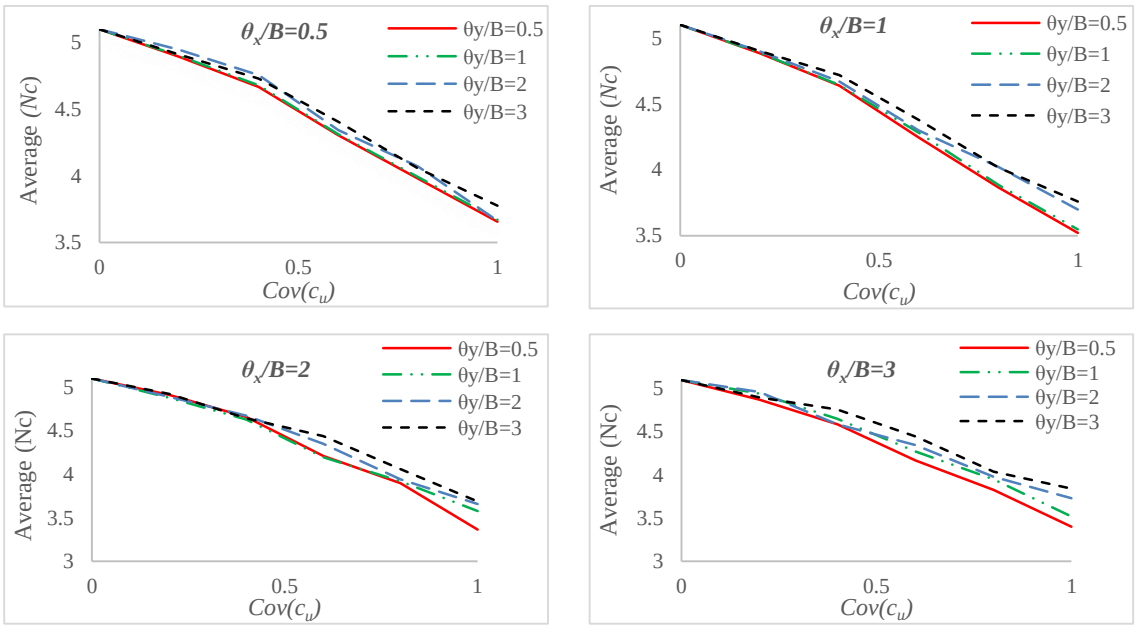

Figure 10. Variations of Average(N_C) vs. variations of Cov(c_u) in different θ_y/B curves

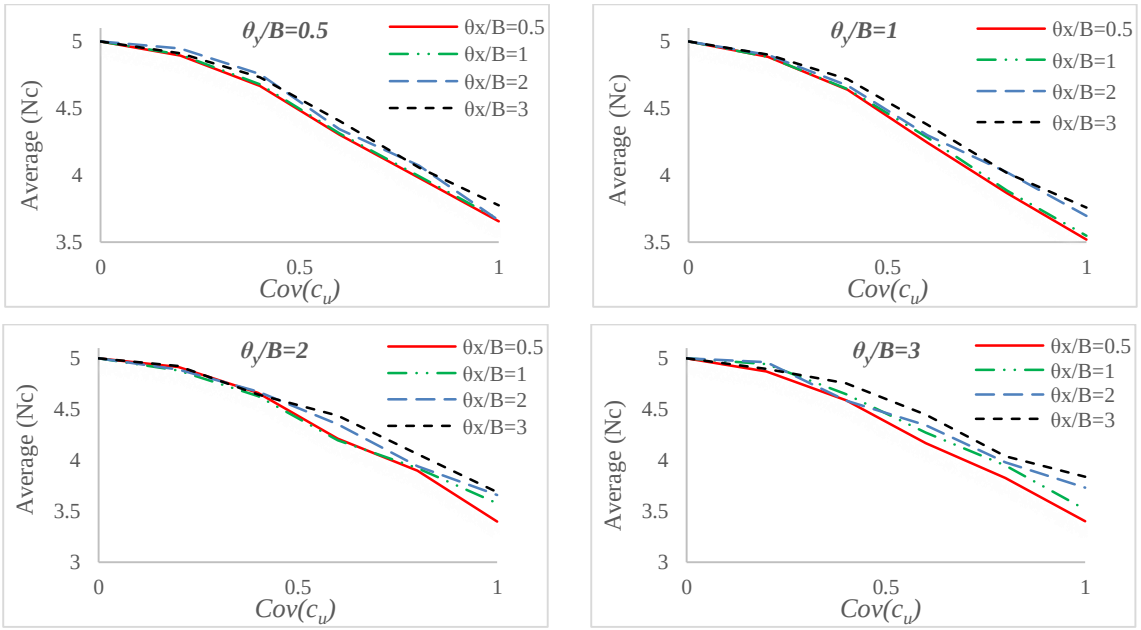

Figure 11. Variations of Average(N_C) vs. variations of Cov(c_u) in different θ_x/B curves

In Figures 12 and 13, the results are drawn in a different form in order to closely inspect the effect of variations in the scales of fluctuation in x and y directions. In Figure 12 and 13 Average(N_C) curves are plotted vs. θ_x/B and θ_y/B respectively for different COV(c_u) values. In Figure 12, it is observed that when θ_y/B is constant ($\theta_y/B = 1$), by growing θ_x/B values from zero, a small decline in Average(N_C) first occurs when θ_x/B is lower than unity; however, when the values of θ_x/B exceed unity, Average(N_C) gradually grow larger with the increase in θ_x/B . In Figure 11, θ_x/B is set to be constant and equal to unity ($\theta_x/B = 1$). It is observed that when θ_x/B is constant, the general trend is the increase in Average(N_C) by growing θ_y/B . This growing trend augments in higher COV(c_u).

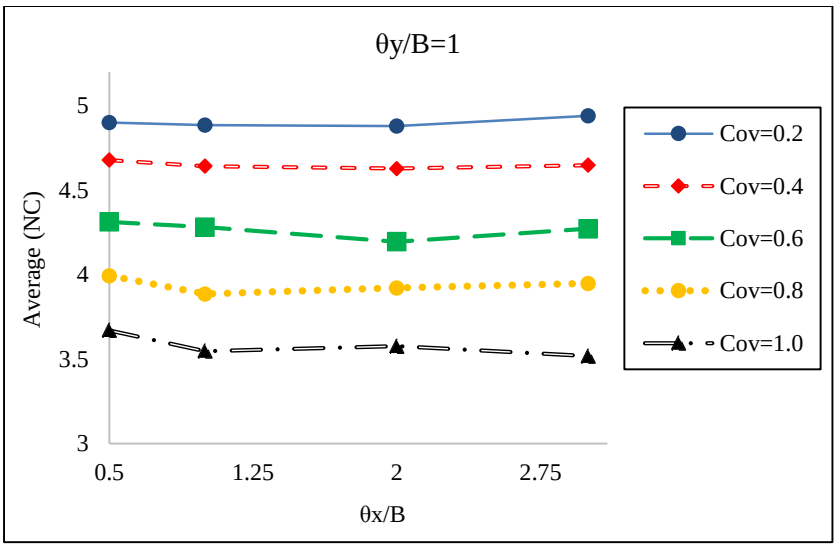

Figure 12. Variation of the Average (N_C) vs. variation of the θ_x/B ratio ($\theta_y/B = 1$)

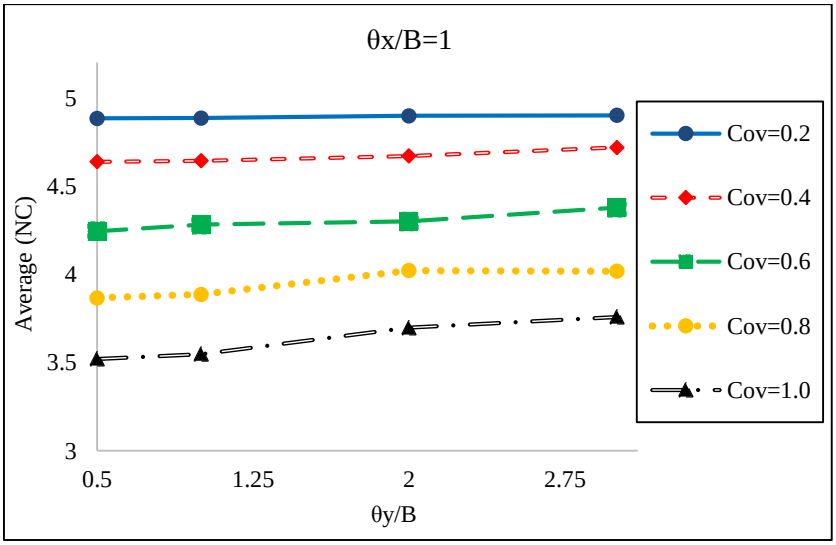

Figure 13. Variation of the Average (N_C) vs. variation of the θ_y/B ratio ($\theta_x/B = 1$)

In Figure 14, the results from the current research are compared with the results of Griffiths et al. (2002). Since scales of fluctuation in both *x* and *y* directions are assumed to be equal in the study by Griffiths et al. (2002), in this figure, the θ parameter which is equal to θ_x and θ_y is used ($\theta = \theta_x = \theta_y$). By observing the resulting charts, it can be interpreted that the general trend in the results of current study is similar to that in former researches.

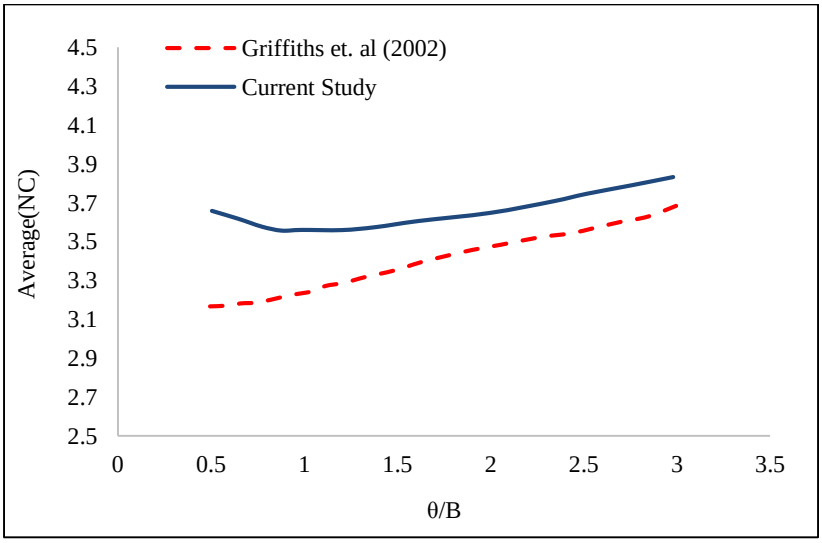

Figure 14. Comparison of results of the current study with the results of Griffith et al. (2002) (Cov(c_u)=1)

5.2. Multiple Regression Analysis

In this study, MRA is implemented to obtain a simple equation to calculate Average (N_C) and COV(N_C). Equation 7 is proposed for computation of Average (N_C). The relevant factors for this equation and the Pearson correlation coefficient (R) are listed in Table 5.

$$Average(N_c) = a1 \times (\theta_x/B\ ) + b1 \times (\theta_y/B) + c1 \times Cov(c_u) + d1 \quad (7)$$

Table 5. The numerical values for the coefficients in equation (7)

Coefficient	Value
a1	0.04666596
b1	-0.013142876
c1	-1.430991893
d1	5.075644975
R	0.99

As shown in Table 5, the R-value is 0.99 for Equation 7. This value indicates the high linear correlation of numerical results with the results from the proposed equation.

In Figure 15, the predicted values for Average (N_C) are plotted versus Average (N_C) from numerical modellings and in Figure 16, residuals of the results of Equation 7 from numerical values are presented in percent. It is observed that the maximum error of Equation 7 is ± 8 in percent. This amount of error is reliable considering the applied statistical procedures, estimations in numerical models and existing uncertainties in shear strength estimations for experimental field problems.

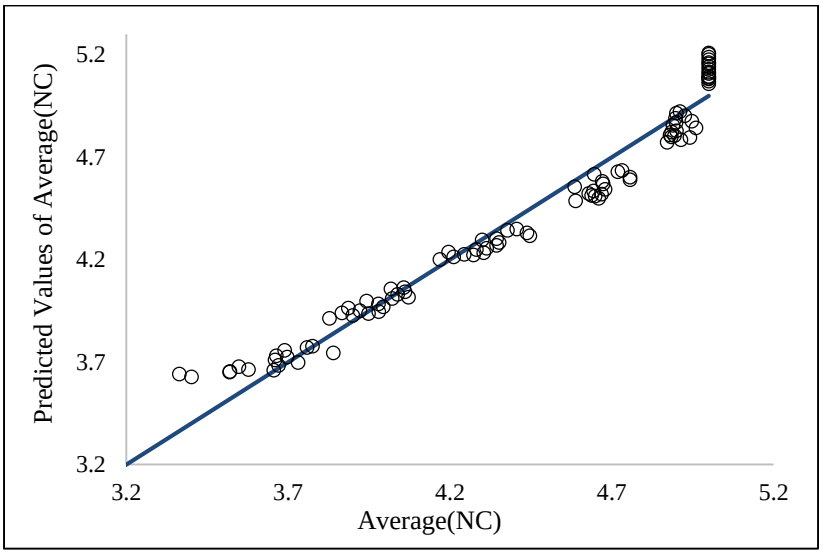

Figure 15. The predicted values for average N_C vs. average N_C from numerical modelling

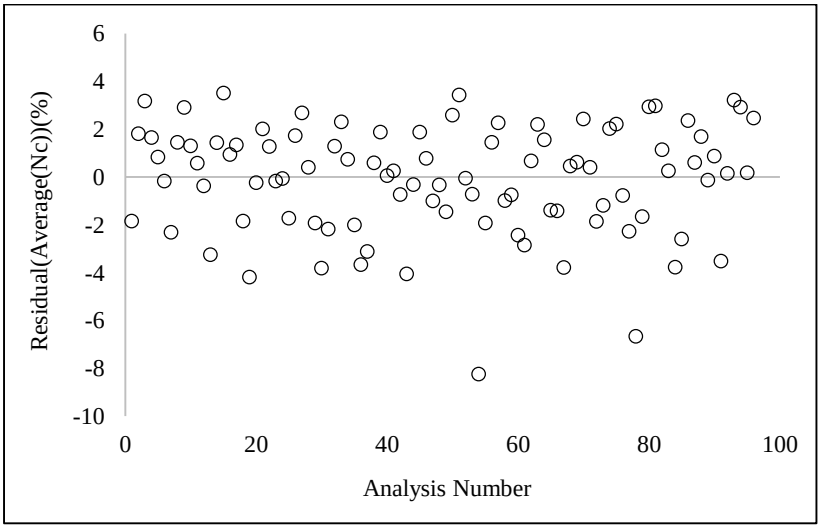

Figure 16. Residuals for the predicted average N_C values and average N_C values from numerical modelling

For computation of the existing uncertainty in Average(N_C), with the knowledge of the spatial variability parameters (i.e., COV(c_u), θ_x/B and θ_y/B), Eq. (8) is proposed. The values for relevant unknown factors in this equation and R-value are listed in Table 6.

$$Cov(N_c) = a2 \times (\theta_x/B\ ) + b2 \times (\theta_y/B) + c2 \times Cov(c_u) + d2 \quad (8)$$

Table 6. The numerical values for the coefficients in Eq. 8

Coefficient	Value
a2	0.044315985
b2	0.028627308
c2	0.432901177
d2	-0.078440695
R	0.96

The graph for the values predicted from Equation 8 for Cov(N_C) versus numerical results is plotted in Figure 17. Figure 18 shows the deviations of the predicted values using Equation 8 with the numerical results. It is observed that the errors of this equation grow when COV(N_C) is lower, especially when COV(N_C) is close to zero. Therefore, when COV(N_C) is trivial, the errors of the Equation 8 grow beyond expectations. However, by considering Figures 17 and 18, it can be deduced that Equation 8 presents reasonable results with tolerable errors when COV(c_u) is between 0.2 and 1.

It is obvious that when COV(N_C) is higher, the scatter in the predicted Average(N_C) from numerical models becomes larger; hence, the design of the footing must be performed using more conservative values of Average(N_C). In other words, when the COV(N_C) grows larger, the designer must use higher safety factor for design of strip footings on nonhomogeneous clays.

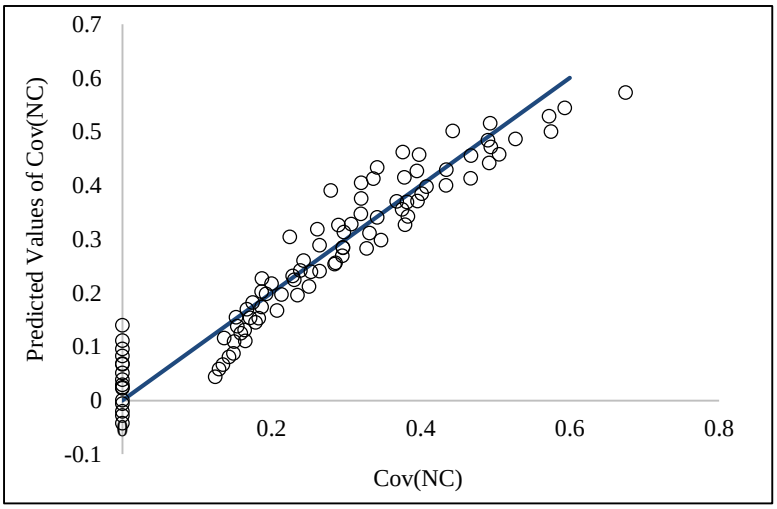

Figure 17. The predicted values for the COV(N_C) vs. the COV(N_C) from numerical modelling

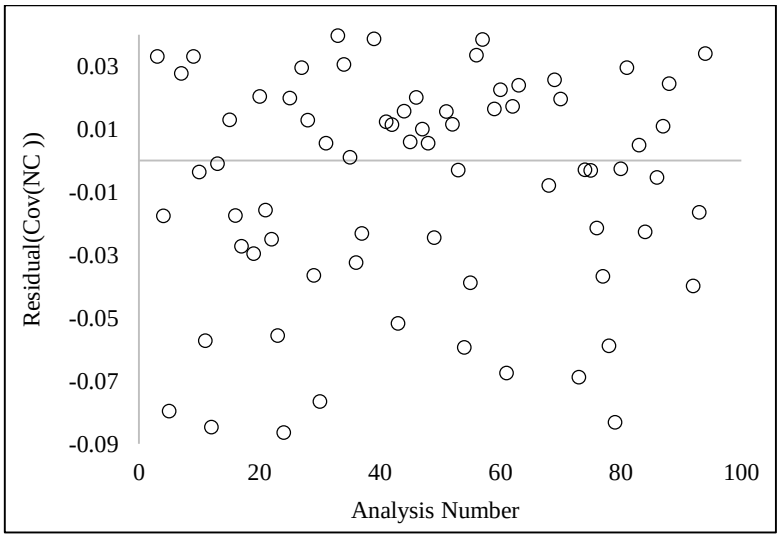

Figure 18. Residuals for the predicted COV(N_C) values and values of the COV(N_C) from numerical modelling

6. Conclusion

In this study, the effect of spatial variability of the undrained shear strength was investigated on the bearing capacity of shallow strip footings. Numerical modelling was performed using the FDM to compute the bearing capacity and to take into account the spatial variability of the undrained shear strength, the random field theory was implemented. The MCS was utilized to generate a distribution from the calculated bearing capacity from numerical models. The mean and COV of the generated distribution were used to assess the effect of spatial variability of the undrained shear strength on the bearing capacity of footings on clays.

The predominant trend in the results was the reduction of the average bearing capacity when the variance of the shear strength increased. By growing the variability of the shear strength in the field, the uncertainty in the calculated average results increases. Thus, more conservatism must be considered when the spatial variation in the field increases. The maximum reduction of undrained bearing capacity by regarding spatial variability of undrained shear strength was observed to be 33.3 percent; thus, the spatial variability of heterogeneous clay could have significant effect on the safe design of footings. Despite the existence of some exceptions, the general trend which was observed in the results is the growing of undrained bearing capacity by the increase in the scales of fluctuation in both x and y directions. Finally, two simple equations were proposed to consider the spatial variability of the shear strength on the bearing capacity of footing on clay layers.

7. Funding

This manuscript presents the results of a research conducted by the authors in a PhD program at Semnan University. The authors received no specific funding for this work.

8. Conflicts of Interest

The authors declare no conflict of interest.

9. References

[1] Vessia, Giovanna, and Savino Russo. "Random Field Theory to Interpret the Spatial Variability of Lacustrine Soils." Biosystems Engineering 168 (April 2018): 4–13. doi:10.1016/j.biosystemseng.2017.08.023.

[2] Gong, Wenping, C. Hsein Juang, James R. Martin, and Lei Wang. "Site Characterization in Geotechnical Engineering—Does a Random Field Model Always Outperform a Random Variable Model?" Geo-Risk 2017 (June 2017). doi:10.1061/9780784480717.046.

[3] Ching, Jianye, Yu-Gang Hu, and Kok-Kwang Phoon. "On Characterizing Spatially Variable Soil Shear Strength Using Spatial Average." Probabilistic Engineering Mechanics 45 (July 2016): 31–43. doi:10.1016/j.probengmech.2016.02.006.

[4] Li, X. Y., L. M. Zhang, and J. H. Li. "Using Conditioned Random Field to Characterize the Variability of Geologic Profiles." Journal of Geotechnical and Geoenvironmental Engineering 142, no. 4 (April 2016): 04015096. doi:10.1061/(asce)gt.1943-5606.0001428.

[5] Gong, Wenping, Yong-Ming Tien, C. Hsein Juang, James R. Martin, and Zhe Luo. "Optimization of Site Investigation Program for Improved Statistical Characterization of Geotechnical Property Based on Random Field Theory." Bulletin of Engineering Geology and the Environment 76, no. 3 (April 1, 2016): 1021–1035. doi:10.1007/s10064-016-0869-3.

[6] Li, Jinhui, Yinghui Tian, and Mark Jason Cassidy. "Failure Mechanism and Bearing Capacity of Footings Buried at Various Depths in Spatially Random Soil." Journal of Geotechnical and Geoenvironmental Engineering 141, no. 2 (February 2015): 04014099. doi:10.1061/(asce)gt.1943-5606.0001219.

[7] Pieczyńska-Kozłowska, J.M., W. Puła, D.V. Griffiths, and G.A. Fenton. "Influence of Embedment, Self-Weight and Anisotropy on Bearing Capacity Reliability Using the Random Finite Element Method." Computers and Geotechnics 67 (June 2015): 229–238. doi:10.1016/j.compgeo.2015.02.013.

[8] Huber, M, P Vermeer, and A Bárdossy. "Evaluation of Soil Variability and Its Consequences." Numerical Methods in Geotechnical Engineering (June 2000): 363–368. doi:10.1201/b10551-68.

[9] Huang, J., Andrei Lyamin, D. Griffiths, Scott Sloan, Kristian Krabbenhoft, and Fenton Ga. "Undrained Bearing Capacity of Spatially Random Clays by Finite Elements and Limit Analysis".(2013).

[10] Griffiths, D. V., and G. A. Fenton. "Bearing Capacity of Spatially Random Soil: The Undrained Clay Prandtl Problem Revisited." Géotechnique 51, no. 4 (May 2001): 351–359. doi:10.1680/geot.2001.51.4.351.

[11] Griffiths, D. V., Gordon A. Fenton, and N. Manoharan. "Bearing Capacity of Rough Rigid Strip Footing on Cohesive Soil: Probabilistic Study." Journal of Geotechnical and Geoenvironmental Engineering 128, no.9 (September 2002): 743–755. doi:10.1061/(asce)1090-0241(2002)128:9(743).

[12] Fenton, G A, and D. V. Griffiths. "Bearing-Capacity Prediction of Spatially Random c - ϕ Soils." Canadian Geotechnical Journal 40, no. 1 (February 2003): 54–65. doi:10.1139/t02-086.

[13] Popescu, Radu, George Deodatis, and Arash Nobahar. "Effects of Random Heterogeneity of Soil Properties on Bearing Capacity." Probabilistic Engineering Mechanics 20, no. 4 (October 2005): 324–341. doi:10.1016/j.probengmech.2005.06.003.

[14] Soubra, Abdul-Hamid, Dalia S. Youssef Abdel Massih, and Mikaël Kalfa. "Bearing Capacity of Foundations Resting on a Spatially Random Soil." GeoCongress 2008 (March 7, 2008). doi:10.1061/40971(310)8.

[15] Kuo, Y.L., M.B. Jaksa, A.V. Lyamin, and W.S. Kaggwa. "ANN-Based Model for Predicting the Bearing Capacity of Strip Footing on Multi-Layered Cohesive Soil." Computers and Geotechnics 36, no. 3 (April 2009): 503–516. doi:10.1016/j.compgeo.2008.07.002.

[16] Srivastava, Amit, and G.L. Sivakumar Babu. "Effect of Soil Variability on the Bearing Capacity of Clay and in Slope Stability Problems." Engineering Geology 108, no. 1–2 (September 2009): 142–152. doi:10.1016/j.enggeo.2009.06.023.

[17] Jamshidi Chenari, Reza, and Ali Mahigir. "The Effect of Spatial Variability and Anisotropy of Soils on Bearing Capacity of Shallow Foundations." Civil Engineering Infrastructures Journal 47, no. 2 (2014): 199-213.

[18] Jamshidi Chenari, Reza, N. Zhalehjoo, and A. Karimian. "Estimation on Bearing Capacity of Shallow Foundations in Heterogeneous Deposits Using Analytical and Numerical Methods." Transactions A: Civil Engineering 21, no. 3 (2014): 505-15.

[19] Ranjbar Pouya, Kaveh, Negin Zhalehjoo, and Reza Jamshidi Chenari. "Influence of Random Heterogeneity of Cross-Correlated Strength Parameters on Bearing Capacity of Shallow Foundations." Indian Geotechnical Journal 44, no. 4 (January 30, 2014): 427–435. doi:10.1007/s40098-013-0096-9.

[20] Griffiths, D. V., Gordon A. Fenton, and N. Manoharan. "Undrained Bearing Capacity of Two-Strip Footings on Spatially Random Soil." International Journal of Geomechanics 6, no. 6 (November 2006): 421–427. doi:10.1061/(asce)1532-3641(2006)6:6(421).

[21] FLAC 7.0. "Reference Manual". Itasca Consulting Group Inc., Minneapolis (2011)

[22] Yockey, Ronald D. "SPSS Demystified" (May 23, 2016). doi:10.4324/9781315508535.

[23] "Foundation Engineering Analysis and Design" (December 6, 2017). doi:10.1201/9781351255400.

[24] Ahmadi, M. M., and B. Mofarraj Kouchaki. "New and Simple Equations for Ultimate Bearing Capacity of Strip Footings on Two-Layered Clays: Numerical Study." International Journal of Geomechanics 16, no. 4 (August 2016): 06015014. doi:10.1061/(asce)gm.1943-5622.0000615.